

Ultrahigh field electron cyclotron resonance absorption in $\text{In}_{1-x}\text{Mn}_x\text{As}$ films

M. A. Zudov* and J. Kono†

*Department of Electrical and Computer Engineering, Rice Quantum Institute
and Center for Nanoscale Science and Technology, Rice University, Houston, Texas 77005*

Y. H. Matsuda,‡ T. Ikaida, and N. Miura

Institute for Solid State Physics, University of Tokyo, Kashiwa, Chiba 277-8581, Japan

H. Munekata

Imaging Science and Engineering Laboratory, Tokyo Institute of Technology, Yokohama, Kanagawa 226-8503, Japan

G. D. Sanders, Y. Sun, and C. J. Stanton

Department of Physics, University of Florida, Gainesville, Florida 32611

(Received 3 July 2002; published 8 October 2002)

We have carried out an ultrahigh-field cyclotron resonance study of n -type $\text{In}_{1-x}\text{Mn}_x\text{As}$ films, with Mn composition x ranging from 0% to 12%, grown on GaAs by low-temperature molecular-beam epitaxy. We observe that the electron cyclotron resonance peak shifts to lower field with increasing x . A detailed comparison of experimental results with calculations based on a modified Pidgeon-Brown model allows us to estimate the s - d and p - d exchange-coupling constants, α and β , for this important III-V dilute magnetic semiconductor system.

DOI: 10.1103/PhysRevB.66.161307

PACS number(s): 76.40.+b, 75.50.Pp, 71.70.Di, 72.25.-b

$\text{In}_{1-x}\text{Mn}_x\text{As}$ alloys and their heterostructures with $\text{Al}_{1-y}\text{Ga}_y\text{Sb}$, the first grown III-V dilute magnetic semiconductor (DMS),¹⁻³ serve as a prototype for implementing electron and hole spin degrees of freedom in semiconductors. Recent experiments have demonstrated the feasibility of controlling ferromagnetism in these systems optically⁴ and electrically.⁵ Understanding their electronic, transport, and optical properties is crucial for designing novel ferromagnetic semiconductor devices with high Curie temperatures. However, their basic band parameters such as effective masses and g factors have not been accurately determined.

The localized Mn spins strongly influence the delocalized conduction- and valence-band states through the s - d and p - d exchange interactions. These interactions are usually parameterized as α and β , respectively.⁶ Determining these parameters is important for understanding the nature of Mn electron states and their mixing with delocalized carrier states. In narrow gap semiconductors like $\text{In}_{1-x}\text{Mn}_x\text{As}$, due to strong interband mixing, α and β can influence *both* the conduction and valence bands. This is in contrast to wide gap semiconductors where α influences primarily the conduction band and β the valence band. In addition, in narrow gap semiconductors, due to the strong interband mixing, the coupling to the Mn spins does not effect all Landau levels by the same amount. As a result, the electron cyclotron resonance (CR) peak can shift as a function of x , the Mn concentration. This can be a sensitive method for estimating these exchange parameters. A recent CR study on $\text{Cd}_{1-x}\text{Mn}_x\text{Te}$ (Ref. 7) showed that the electron mass is strongly affected by sp - d hybridization. To our knowledge, however, there have been no CR studies on any III-V DMS systems (for our preliminary results, see Refs. 8, 9).

In this paper we describe the dependence of electron CR observed in n -type $\text{In}_{1-x}\text{Mn}_x\text{As}$ films on x . A detailed com-

parison with theoretical calculations provides insight into the effects of Mn ions on the Landau and Zeeman splittings of the conduction-band states.

We studied four ~ 2 - μm -thick $\text{In}_{1-x}\text{Mn}_x\text{As}$ films with $x=0, 0.025, 0.050$, and 0.120 by ultrahigh-field magnetoabsorption spectroscopy. The films were grown by molecular-beam epitaxy on semi-insulating GaAs substrates at 200°C . All the samples were of n type and did not show ferromagnetism down to 1.5 K. The electron densities and mobilities deduced from Hall measurements are listed in Table I. The single-turn coil technique¹⁰ was used to generate ultrahigh magnetic fields with pulse duration ~ 7 μs . The sample and the pickup coil were placed in a liquid-helium flow cryostat. We used the 10.6 - μm line from a CO_2 laser and produced circular polarization using a CdS quarterwave plate. The transmitted radiation was detected by a fast HgCdTe photovoltaic detector.

Typical measured CR spectra at 30 K and 290 K are shown in Figs. 1(a) and 1(b), respectively. Note that to compare the transmission with absorption calculations, the trans-

TABLE I. Densities, mobilities, and cyclotron masses for the four samples studied. The densities and mobilities are in units of cm^{-3} and cm^2/Vs , respectively. The masses were obtained at a photon energy of 117 meV (or $\lambda = 10.6$ μm).

Mn content x	0	0.025	0.050	0.120
Density (4.2 K)	$\sim 1.0 \times 10^{17}$	1.0×10^{16}	0.9×10^{16}	1.0×10^{16}
Density (290 K)	$\sim 1.0 \times 10^{17}$	2.1×10^{17}	1.8×10^{17}	7.0×10^{16}
Mobility (4.2 K)	~ 4000	1300	1200	450
Mobility (290 K)	~ 4000	400	375	450
m/m_0 (30 K)	0.0342	0.0303	0.0274	0.0263
m/m_0 (290 K)	0.0341	0.0334	0.0325	0.0272

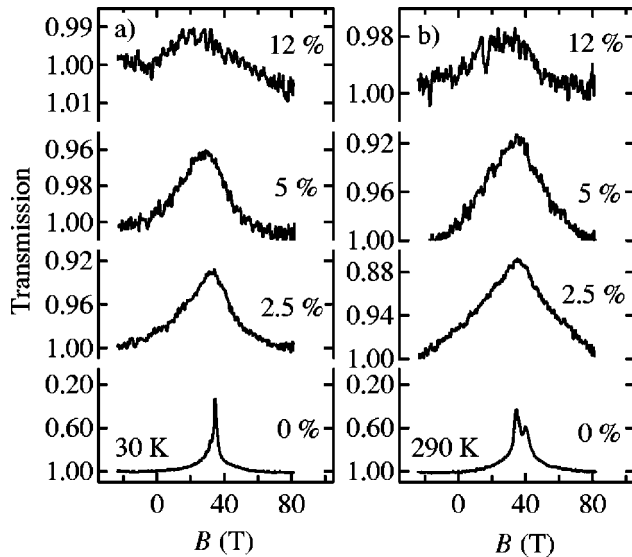


FIG. 1. Experimental CR spectra for different Mn contents taken at 290 (a) and 30 K (b). The wavelength of the laser was fixed at $10.6 \mu\text{m}$ with electron-active circular polarization while the magnetic field B was swept. The resonance position shifts to lower B with increasing x . The x values are 0%, 2.5%, 5%, and 12%.

mission increases in the negative \hat{y} direction. Each figure shows spectra for all four samples labeled by the corresponding Mn compositions from 0% to 12%. All the samples show pronounced absorption peaks (or transmission dips) and the resonance field *decreases* with increasing x . Increasing x from 0% to 12% results in a $\sim 25\%$ decrease in cyclotron mass (see Table I). It is important to note that at reso-

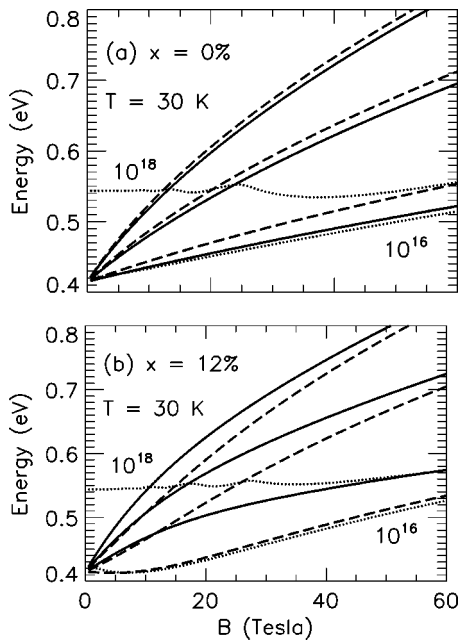


FIG. 2. Electron Landau levels as a function of the magnetic field B at 30 K for (a) $x=0\%$ and (b) $x=12\%$. Spin-up (-down) levels are shown as solid (dashed) lines. The Fermi levels are indicated by dotted lines for electron concentrations of 10^{16} and 10^{18}cm^{-3} .

nance, the densities and fields are such that only the lowest Landau level for each spin type is occupied (see Fig. 2). Thus, all the electrons were in the lowest Landau level for a given spin even at room temperature, precluding any density-dependent mass due to nonparabolicity (expected at zero or low magnetic fields) as the cause of the observed trend.

At high temperatures [e.g., Fig. 1(b)], the $x=0$ sample clearly shows nonparabolicity-induced CR spin splitting with the weaker (stronger) peak originating from the lowest spin-down (spin-up) Landau level, while the other three samples do not show such splitting. The reason for the absence of splitting in the Mn-doped samples is a combination of 1) their low mobilities (which lead to substantial broadening) and 2) the large effective g factors due to the Mn ions; especially in samples with large x , only the spin-down level is substantially thermally populated (cf. Fig. 2).

We also performed mid-infrared interband absorption measurements at various temperatures using Fourier-transform infrared spectroscopy, which revealed no significant x dependence of the band gap except for the different amounts of Burstein-Moss shifts due to the different carrier densities.

We calculated the conduction-band Landau levels based on a modified Pidgeon-Brown model^{11,12} including full k_z dependence and also $sp-d$ exchange coupling of the electrons and holes to the Mn ions. This is a 8×8 band $\mathbf{k} \cdot \mathbf{p}$ method with a magnetic field along the [001] direction. We used a standard set of band parameters for InAs,¹³ neglecting any x dependence of these parameters. We vary the gap with T according to $E_g(T) = 0.417 - 0.000276T^2/(93+T)$ eV.¹³ As seen in Table I, the mass does not vary significantly with T . Other low field CR studies of InAs (Ref. 14) show a very weak T dependence to the cyclotron mass and also take into account the polaron effects. Since we are mainly interested in the x dependence of the mass, for simplicity, we adjust the F parameter to keep the mass constant with T . Alternatively, one might wish to keep F constant and vary the $\mathbf{k} \cdot \mathbf{p}$ optical matrix element E_p .

Since $\text{In}_{1-x}\text{Mn}_x\text{As}$ is a narrow gap semiconductor, the coupling between the valence and conduction bands is strong, and thus, not only α but also β is important in calculating the conduction-band Landau levels. A photoemission experiment¹⁵ reports $\beta = -0.7$ eV, and a theoretical estimate¹⁶ suggests that $\beta \approx -0.98$ eV. No value has been reported for α , to our knowledge.

We chose $\beta = -1.0$ eV and $\alpha = 0.5$ eV as the values that best represent the observed trends, though these values can change depending upon the other parameters used in the $\mathbf{k} \cdot \mathbf{p}$ calculation. Figures 2(a) and 2(b) show the lowest three Landau levels (spin up and down) in the conduction band for the $x=0$ and 12% samples. In addition, the Fermi levels are calculated and plotted (dotted lines) for carrier densities of 10^{18}cm^{-3} and 10^{16}cm^{-3} . Both the mass and the g factor are strongly energy dependent, magnetic-field dependent, as well as x dependent. We can also see that in the $x=12\%$ sample, the *spin order is reversed* and the spin splitting is significantly enhanced by the presence of Mn ions; the latter explains the absence of CR spin splitting in the 12% sample. We found that both the sign and values of α and β are

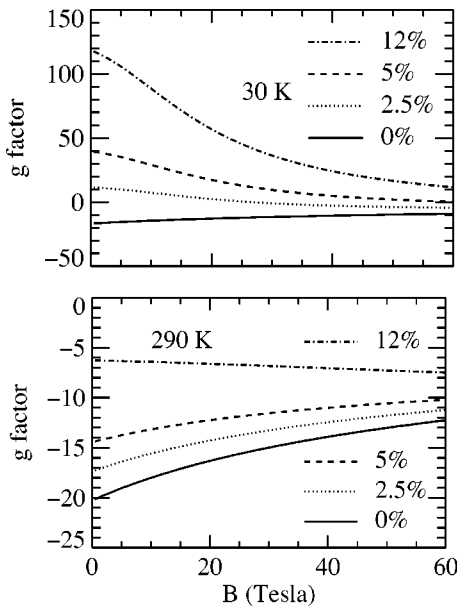


FIG. 3. Electron effective g factors for $\text{In}_{1-x}\text{Mn}_x\text{As}$ as a function of applied magnetic field for several values of Mn concentration x . The upper and lower panels correspond to $T=30$ K and $T=290$ K, respectively.

critically important in explaining the experimental data and therefore it is a good method for determining these parameters. In various investigations of II-VI DMS's it has been established that α and β differ in sign, and usually the absolute value of β is greater than α ,^{6,12} which is consistent with our results.

In Fig. 3, we show the effective g factors for electrons in the lowest Landau level in $\text{In}_{1-x}\text{Mn}_x\text{As}$ as a function of applied magnetic field for different Mn-doping concentrations x . The curves are shown for temperatures of 30 K and 290 K, respectively. As can be seen, at 30 K and high Mn concentration, the effective g factor is extremely large (>100) and has the sign opposite to that of the undoped sample. Due to Mn doping and the large nonparabolicity of the narrow gap semiconductor, the g factor is very dependent on magnetic field, and is reduced substantially at high magnetic fields and temperatures.

Based on the calculated Landau levels, we also calculated the cyclotron resonance spectra for the four samples at 30 K and 290 K. The magneto-optical absorption coefficient at the photon energy $\hbar\omega$ is¹⁷

$$\alpha(\hbar\omega) = \frac{\hbar\omega}{(\hbar c)n_r} \epsilon_2(\hbar\omega), \quad (1)$$

where $\epsilon_2(\hbar\omega)$ is the imaginary part of the dielectric function and n_r is the index of refraction. The imaginary part of the dielectric function is found using Fermi's golden rule. The result is

$$\epsilon_2(\hbar\omega) = \frac{e^2}{\lambda^2(\hbar\omega)^2} \sum_{n,\nu;n',\nu'} \int_{-\infty}^{\infty} dk_z |\hat{e} \cdot \vec{P}_{n,\nu}^{n',\nu'}(k_z)|^2 \times (f_{n,\nu}(k_z) - f_{n',\nu'}(k_z)) \delta[\Delta E_{n,\nu}^{n',\nu'}(k_z) - \hbar\omega], \quad (2)$$

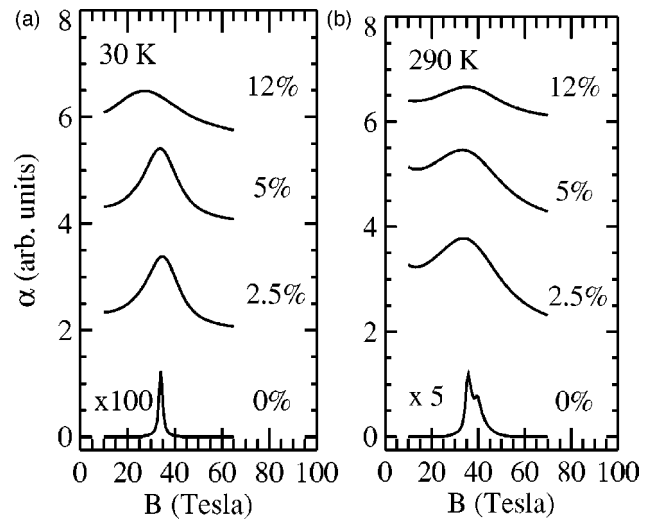


FIG. 4. Calculated CR absorption as a function of magnetic field at 30 K (a) and 290 K (b). The curves were calculated based on the Pidgeon-Brown model and the golden rule for absorption. The curves were broadened based on the mobilities reported in Table I.

where $\Delta E_{n,\nu}^{n',\nu'}(k_z) = E_{n',\nu'}(k_z) - E_{n,\nu}(k_z)$ is the transition energy and $\lambda = \sqrt{\hbar c/eB}$ is the magnetic length. The function $f_{n,\nu}(k_z)$ in Eq. (2) is the probability that the state (n,ν,k_z) , with energy $E_{n,\nu}(k_z)$, is occupied. It is given by the Fermi distribution function, and depends on the net carrier density.

Figures 4(a) and 4(b) show the calculated CR absorption coefficient for electron-active circularly polarized 10.6- μm light in the Faraday configuration as a function of magnetic field at 30 K and 290 K, respectively. Densities for each sample are given in Table I. In the calculation, the curves were broadened based on the mobilities of the samples. The broadening used for $T=30$ K was 4 meV for 0%, 40 meV for 2.5%, 40 meV for 5%, and 80 meV for 12%. For $T=290$ K, the broadening used was 4 meV for 0%, 80 meV for 2.5%, 80 meV for 5%, and 80 meV for 12%.

At $T=30$ K, we see a shift in the CR peak as a function of doping in agreement with Fig. 1(a). For $T=290$ K, we see the presence of two peaks in the pure InAs sample. The second peak originates from the thermal population of the lowest spin-down Landau level (cf. Fig. 2). The peak does not shift as much with doping, as it did at low temperature. This results from the temperature dependence of the average Mn spin. We believe that the Brillouin function used for calculating the average Mn spin becomes inadequate at large x and/or high temperature due to its neglect of Mn-Mn interactions, such as pairing and clustering.

In summary, we have observed electron CR in $\text{In}_{1-x}\text{Mn}_x\text{As}$ and studied its dependence on the Mn concentration x . Owing to band mixing in this narrow gap system, the CR peak actually shifts with x ; we observed a $\sim 25\%$ mass reduction by increasing x from 0 to 0.12. Theoretical calculations based on a 8×8 band $\mathbf{k} \cdot \mathbf{p}$ model successfully reproduce this behavior. These results demonstrate that CR can be used for determining the $sp-d$, (electron/hole)-Mn ion exchange interactions α and β . We obtained $\beta = -1.0$ eV

and $\alpha=0.5$ eV as the values which best represent the observed trends. We also showed that at low temperatures and high x , the effective g factor is extremely large (>100) and has the sign opposite to that of the $x=0$ sample; it is very dependent on magnetic field and is reduced substantially at high magnetic fields and temperatures. These findings should

be useful for designing novel spin-based semiconductor devices.

This work was supported by the DARPA through Grant No. MDA972-00-1-0034 and the NEDO International Joint Research Program.

*Present address: Physics Department, University of Utah, Salt Lake City, Utah 84112.

†To whom correspondence should be addressed. Electronic address: kono@rice.edu; <http://www.ece.rice.edu/~kono>

‡Present address: Department of Physics, Faculty of Science, Okayama University, Okayama, Japan.

¹H. Munekata, H. Ohno, S. von Molnar, A. Segmuller, L.L. Chang, and L. Esaki, *Phys. Rev. Lett.* **63**, 1849 (1989).

²H. Munekata, H. Ohno, R.R. Ruf, R.J. Gambino, and L.L. Chang, *J. Cryst. Growth*, **111**, 1011 (1991); H. Ohno, H. Munekata, T. Penney, S. von Molnar, and L.L. Chang, *Phys. Rev. Lett.* **68**, 2664 (1992).

³H. Munekata, A. Zaslavsky, P. Fumagalli, and R.J. Gambino, *Appl. Phys. Lett.* **63**, 2929 (1993).

⁴S. Koshihara, A. Oiwa, M. Hirasawa, S. Katsumoto, Y. Iye, C. Urano, H. Takagi, and H. Munekata, *Phys. Rev. Lett.* **78**, 4617 (1997); A. Oiwa, T. Slupinski, and H. Munekata, *Appl. Phys. Lett.* **78**, 518 (2001).

⁵H. Ohno, D. Chiba, F. Matsukura, T. Omiya, E. Abe, T. Dietl, Y. Ohno, and K. Ohtani, *Nature (London)* **408**, 944 (2000).

⁶J.K. Furdyna, *J. Appl. Phys.* **64**, R29 (1988).

⁷Y.H. Matsuda, T. Ikaida, N. Miura, S. Kuroda, F. Takano, and

K. Takita, *Phys. Rev. B* **65**, 115202 (2002).

⁸Y.H. Matsuda, T. Ikaida, N. Miura, M.A. Zudov, J. Kono, and H. Munekata, *Physica E (Amsterdam)* **10**, 219 (2001).

⁹Y.H. Matsuda, T. Ikaida, N. Miura, Y. Hashimoto, S. Katsumoto, M.A. Zudov, J. Kono, and H. Munekata, in *Proceedings of the Tenth International Conference on Narrow Gap Semiconductors*, edited by N. Miura, S. Yamada, and S. Takeyama (Institute of Pure and Applied Physics, Tokyo, 2001), pp. 93–95.

¹⁰K. Nakao, F. Herlach, T. Goto, S. Takeyama, T. Sakakibara, and N. Miura, *J. Phys. E* **18**, 1018 (1985).

¹¹C.R. Pidgeon and N.R. Brown, *Phys. Rev.* **146**, 575 (1966).

¹²J. Kossut, *Semicond. Semimetals* **25**, 183 (1988).

¹³I. Vurgaftman, J.R. Meyer, and L.R. Ram-Mohan, *J. Appl. Phys.* **89**, 5815 (2001).

¹⁴E.D. Palik and R.F. Wallis, *Phys. Rev.* **123**, 131 (1961).

¹⁵J. Okabayashi, T. Mizokawa, D.D. Sarma, A. Fujimori, T. Slupinski, A. Oiwa, and H. Munekata, *Phys. Rev. B* **65**, 161203 (2002).

¹⁶T. Dietl, H. Ohno, and F. Matsukura, *Phys. Rev. B* **63**, 195205 (2000).

¹⁷F. Bassani and G.P. Parravicini, *Electronic States and Optical Transitions in Solids* (Pergamon, New York, 1975).